Eur. Phys. J. B **58**, 483–491 (2007)
DOI: 10.1140/epjb/e2007-00238-8

THE EUROPEAN PHYSICAL JOURNAL B

Linear response in aging glassy systems, intermittency and the Poisson statistics of record fluctuations

P. Sibani[a]

Institut for Fysik og Kemi, SDU, 5230 Odense M, Denmark

Received 30 November 2006 / Received in final form 18 May 2007
Published online 14 September 2007 –

Abstract. We study the intermittent behavior of the energy decay and the linear magnetic response of a glassy system during isothermal aging after a deep thermal quench, using the Edward-Anderson spin glass model as a paradigmatic example. The large intermittent changes in the two observables occur in a correlated fashion and through irreversible bursts, 'quakes', which punctuate reversible and equilibrium-like fluctuations of zero average. The temporal distribution of the quakes is a Poisson distribution with an average growing logarithmically on time, indicating that the quakes are triggered by record sized fluctuations. As the drift of an aging system is to a good approximation subordinated to the quakes, simple analytical expressions [Sibani et al. Phys Rev B **74**, 224407 (2006)] are available for the time and age dependence of the average response and average energy. These expressions are shown to capture the time dependencies of the EA simulation results. Finally, we argue that whenever the changes of the linear response function and of its conjugate autocorrelation function follow from the same intermittent events a fluctuation-dissipation-like relation can arise between the two in off-equilibrium aging.

PACS. 65.60.+a Thermal properties of amorphous solids and glasses – 05.40.-a Fluctuation phenomena, random processes, noise, and Brownian motion – 61.43.Fs Glasses – 75.10.Nr Spin-glass and other random models

1 Motivation

In noise spectra from mesoscopic aging systems, reversible fluctuations are punctuated by rare and large, so called intermittent, events [1–6], which arguably signal switches from one metastable configuration to another [7,8]. The intermittent events usually appear as an exponential tail in the Probability Density Function (PDF) of the fluctuations. The central part of the PDF describes equilibrium-like behavior with its zero-centered Gaussian shape. Exploiting this information can add new twists to long debated issues as the multiscale nature of glassy dynamics and the associated memory behavior.

A *record dynamics* scenario for aging [8–10] builds on two main assumptions: *(i)* record sized energy fluctuations within metastable domains trigger *irreversible* intermittent events, or *quakes*; *(ii)* these, in turn, control all significant physical changes, e.g. heat release, configurational decorrelation and linear magnetic response. In brief, all important changes are considered to be *subordinated* to the quakes, with the latter triggered by energy fluctuations of *record* size. Combining the information from the equilibrium-like fluctuations with non-thermal properties, e.g. irreversible energy losses, leads to testable predictions for the time and temperature dependencies of the fluctuation spectra which have been confirmed in a number of cases [8,11–16].

While macroscopic (average) linear response functions have long been the tool of choice for probing aging in magnetic systems, [17–21], the predictions of record dynamics have so far only been tested for experimental Thermoremanent Magnetization (TRM) spin glass data [16]. Simulations offer certain advantages over experiments: it is possible to simulate an instantaneous quench, simply by choosing a 'random', i.e. high temperature, initial condition. Notably, an instantaneous initial quench leads to the 'full aging' [20], scaling behavior simply explained in record dynamics; secondly, the statistical analysis is considerably simplified when thousands of independent traces can be generated; lastly, temporal correlations between the intermittent changes of the magnetization and the energy can be extracted.

The Edwards-Anderson (EA) spin-glass model used in this work is a paradigmatic example of an aging system. Its macroscopic (average) magnetic response and autocorrelation decay have been thoroughly investigated [22–25] and its mesoscopic fluctuations properties have attracted some recent attention [8,13,26]. Here, data from extensive simulations are analyzed with focus on the intermittency

[a] e-mail: paolo.sibani@fys.sdu.dk

of the energy and Zero Field Cooled Magnetization (ZFCM) fluctuations We confirm that quakes carry the net drift of the energy [8] and correlate strongly with the large intermittent magnetization fluctuations carrying the net change of the linear response. The idea [8,10] that quakes have a Poisson distribution with a *logarithmic* time dependence is derived from record statistics and is central to the theory. To verify it empirically, we consider the temporal statistics of the difference of 'logarithmic waiting times' $\log(t_q) - \log(t_{q-1})$, where t_q marks the occurence of the qth quake in a given trace. For the above Poisson distribution, these logarithmic differences are exponentially distributed. General mathematical arguments lead to eigenvalue expansions for the dependence of the average energy and linear response on the number of quakes, and then, via the subordination hypothesis, to power-law expansions for the time dependences of the same quantities [13,16]. The expansions are tested below against the EA model numerical simulation results. The origin of approximate off-equilibrium Fluctuation-Dissipation like relations is discussed in the last section from the point of view of record dynamics.

Finally, a notational issue: as in reference [16], the variable t generically denotes the time elapsed from the initial quench, i.e. the system age. The external field is switched on at time $t = t_w$, and $t_{obs} = t - t_w$ denotes the observation time, a quantity called t in references [8,13] and in many experimental papers, e.g. [27,20]. Unless otherwise stated, we denote the *average* energy and magnetization by μ_e and μ_{ZFCM}, and reserve the symbols e and M for the corresponding fluctuating quantities measured in the simulations. The simulation temperature is denoted by T.

2 Model and simulation methods

In the Edwards-Anderson model, N Ising variables, $\sigma_i = \pm 1$, are placed on a cubic lattice with toroidal boundary conditions. Their interaction energy is

$$E = -\frac{1}{2}\sum_{i,j}^{N} \sigma_i \sigma_j J_{ij} - H \sum_{i}^{N} \sigma_i, \qquad (1)$$

where $\sum_i \sigma_i = M$ is the magnetization and H is the magnetic field. The non-zero elements of the symmetric interaction matrix J_{ij} connect neighboring sites on the lattice. The interactions are drawn from a Gaussian distribution with zero average and unit variance, a choice setting the scale for both temperature and magnetic field.

In the simulations, we use system size $N = 16^3$ and collect the statistics of energy and magnetization changes from several thousands of independent trajectories, each corresponding to a different realization of the J_{ij}'s. After the initial quench, aging procedes isothermally in zero field untill time $t = t_w$, where a small magnetic field $H = 0.1$ is instantaneously turned on. Isothermal simulations lasting up to age $t = 100\, t_w$ are carried out for $t_w = 50, 100, 200, 500$ and 1000 at temperatures $T = 0.1, 0.2, \ldots 0.8$. The simulation engine utilizes the Waiting Time Method [15,28] a rejectionless or 'event driven' algorithm which operates with an 'intrinsic' time, loosely corresponding to a sweep of the Metropolis algorithm. Unlike the Metropolis algorithm, the WTM can follow spatio-temporal patterns on very short time scales, a property advantageous for intermittency studies.

3 Simulation results

In this section, simulation results are presented together with some relevant theoretical considerations. The first subsection deals with the distribution of energy and magnetization changes, δE and δM, occurring over small intervals δt. The Probability Density Function (PDF) of these quantities characterizes intermittency in the EA model in a simple and direct way. In the second subsection, the quakes are (approximately) identified within each data stream, and the temporal aspects of their distribution are studied. In the third and last subsection, the average linear response and average energy obtained from the simulations are compared to analytical predictions which are based on the temporal distribution of the quakes.

3.1 Energy and magnetization fluctuation statistics

For a first statistical description of the energy and the ZFCM fluctuations, energy and magnetization changes δE and δM occurring over small intervals δt are sampled during the time interval $[1000, 3000]$. The left panel of Figure 1 shows the PDF of the magnetic fluctuations (blue circles) on a log scale. The (black) line is the fit to a zero-centered Gaussian obtained using data within the interval $-80 < \delta M < 50$. The distribution of the remaining large positive magnetization changes is seen to have exponential character. The same runs are used to collect the PDF of the energy fluctuations, shown in the right panel of Figure 1 (lower data set, blue circles). Again, we see a combination of a zero centered Gaussian and an intermittent exponential tail. The full line is a fit to the zero centered Gaussian in the interval $-5 < \delta E < 20$.

As intermittent fluctuations are rare, the temporal correlation between intermittent energy and ZFC magnetization changes is best observed using conditional PDF's (upper curve, red squares). The conditional PDF shown only includes those δE values which either fall in the same or the preceding interval of width δt as magnetic fluctuations above the threshold $\delta M = 50$. In the left panel of the figure, the threshold is seen to be near the boundary between reversible and intermittent magnetization changes. Note how the Gaussian parts of the full and of the conditional PDFs nearly coincide, while the corresponding intermittent tails differ. The tail of the conditional PDF is strongly enhanced (roughly, between 10 and 100 times) when only fluctuations near a large magnetization change are included in the count. A similar situation is observed at any low temperatures.

Figure 2 details the dependence of the PDF of the magnetization fluctuations on δt and T: the three PDFs shown in the left panel of Figure 2 as green circles, blue

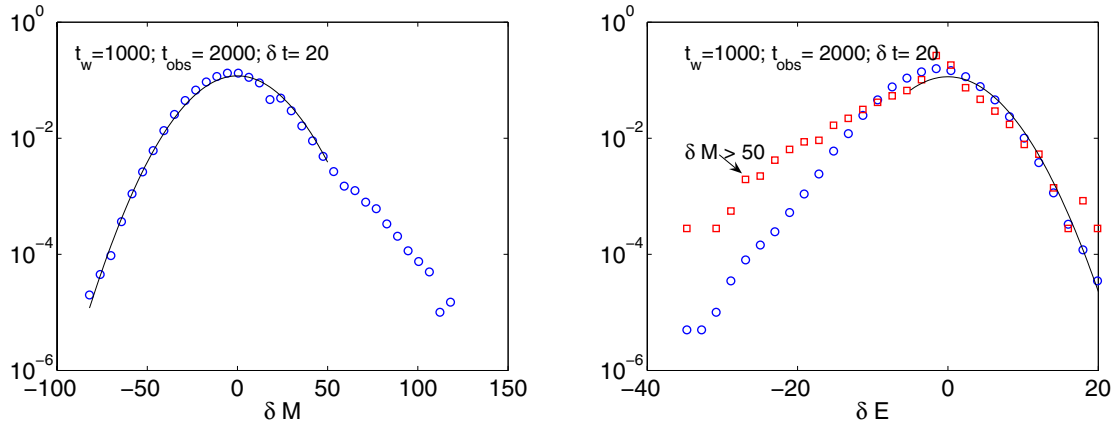

Fig. 1. (Color on line) The left panel shows the PDF (blue circles) of the magnetization changes δM occurring over intervals of length $\delta t = 20$ during isothermal simulations at temperature $T = 0.4$. The statistics is based on 2×10^5 data points obtained in the age interval $[1000, 3000]$ using 2000 independent trajectories. The zero average Gaussian (black line) fits data points with $-80 < \delta M < 50$. The right panel shows the PDF of the energy changes (blue circles), and a Gaussian fit of the positive energy fluctuations (black line). The red squares pertain to the subset of energy changes occurring in the immediate vicinity of large ($\delta M > 50$) magnetization changes. All data are obtained from the same set of trajectories as those shown in the left panel.

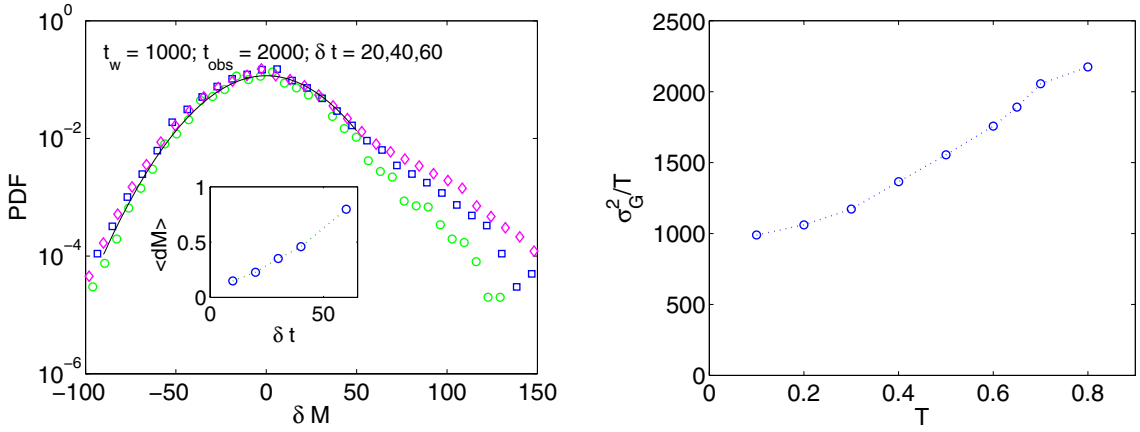

Fig. 2. (Color on line) The left panel depicts the PDF of the magnetization changes δM over intervals of length δt. The simulation temperature is $T = 0.4$. Green circles, blue squares and magenta diamonds correspond to $\delta t = 20, 40$ and 60, respectively. The data are collected in the interval $[1000, 3000]$. In order of increasing δt, the statistics is based on 10^5, $.5 \times 10^5$ and $.33 \times 10^5$ data points. The full line is a fit of all data with $-80 < \delta M < 50$ to a Gaussian centered at zero. For $\delta M > 50$ the PDF clearly deviates from a Gaussian shape. The intermittent tail grows with δt and fully determines the average change in the ZFC magnetization. The insert shows dM, averaged over t_{obs}, versus δt. The right panel shows the variance of the (fitted) Gaussians as a function of the reduced temperature T/T_g.

squares and magenta diamonds are obtained in the interval $[1000, 3000]$, for $T = 0.4$ and for $\delta t = 20, 40$ and 60, respectively. The black line is a zero centered Gaussian fitted to the PDF in the range $-80 < \delta M < 10$. The fit is obtained by optimizing the variance of the Gaussian distribution, σ_G^2. The latter quantity should not be confused with the variance of the full distribution, which is much larger and heavily influenced by the tail events excluded from the Gaussian fit. Importantly, since the Gaussian part of the PDF is independent of δt quasi-equilibrium ZFCM fluctuations at $T = 0.4$ can be treated as uncorrelated for times larger than $\delta t = 20$. Secondly, since the Gaussian is centered at zero, any changes in the average magnetization are exclusively due to the intermittent events. Similar conclusions were reached for the spin-glass TRM magnetization [16], and for the energy outflow in the EA model [8], and in a p-spin model with no quenched randomness [15]. The insert describes the dependence on δt of the magnetization change $\langle \delta M \rangle$ averaged over the observation interval $[1000, 3000]$. E.g. the data point corresponding to $\delta t = 20$ depicts the average of the lowest PDF plotted in the main figure. The right panel of Figure 2 shows a plot of the ratio σ_G^2/T versus T for the Gaussian part of the magnetic fluctuations. As the Fluctuation-Dissipation Theorem (FDT) applies to the equilibrium-like part of the dynamics, the ordinate can be interpreted as the (gedanken) linear

magnetic susceptibility of metastable configurations. The overall shape of the curve is reminiscent of the experimental T dependence of the ZFCM below T_g [29].

3.2 Temporal distribution of intermittent events

The PDF of intermittent fluctuations in the EA model scales with the ratio $\delta t/t$, where t is the age of the system at the beginning of the sampling interval [8]. The rate of quakes accordingly decays as the inverse of the age, in agreement with the claim that the the number of independent quakes in an interval (t, t') has a Poisson distribution with average $\langle n_I \rangle = \alpha \log(t/t')$ The parameter α characterizing the average is interpreted as the number of thermalized domains contributing in parallel to the fluctuation statistics. This quantity is expected to be temperature independent and linearly dependent on system size [15]. Using that the differences $\tau_q = \log(t_q) - \log(t_{q-1}) = \log(t_q/t_{q-1})$ are independent random numbers, all exponentially distributed with the same average $\langle \tau_q \rangle = 1/\alpha$, identifying the times t_q, $q = 1, 2, \ldots$ at which the quakes occur allows one to check the temporal aspects of statistics (as opposed to the distribution of quake sizes).

The identification entails some challenges of statistical and patter-recognition nature. The residence times $t_q - t_{q-1}$ expectedly have a broad distribution [10], which, in connection with a finite sampling time creates a negative sampling bias on large t_q values [11], even with the quakes unambiguously identified. Secondly, correlations may well be present between large and closely spaced spikes in the signal which collectively represent a change of attractor. Last but not least, identification of the t_q's within a trace must rely on the negative sign of the fluctuations and on their 'sufficiently large' size. I.e. by definition sufficient energy must be released to make the reverse process highly unprobable within an observation span stretching up to $2t$ for a quake which occurs at t [10]. A related and generic property of aging systems (also directly accessible by an intermittency analysis [8]) is that reversible equilibrium-like fluctuations dominate the dynamics on time scales shorter than the age t. A simple empirical criterion for distinguishing reversible fluctuations from irreversible quakes uses an upper bound on the probability, $P_{rev}(t, \delta E)$, that at least one thermal energy fluctuation of positive sign be among $t/\delta t$ observations. For small $\exp(-\delta E/T)$, $P_{rev}(t, \delta E) \approx t/\delta t c \exp(-\delta E/T)$, where the positive number c is unknown. A negative energy fluctuation is labeled as a quake if its absolute value $|\delta E|$ satisfies $P_{rev}(t, |\delta E|) < 10^{-n}$, where n is a positive number. For a thermal fluctuation which occurs at age t, this criterion produces the inequality

$$\frac{|\delta E|_{\text{quake}}}{T} > f + \log t; \quad \text{where} \quad f = n \ln(10) + \ln(c/\delta t). \tag{2}$$

The formal definition of the 'filter' parameter f on the right hand side of the inequality contains the unknown parameter c as well as a free parameter n. We must therefore treat f as a free parameter regulating how strict a filter the fluctuations must pass to qualify as quakes.

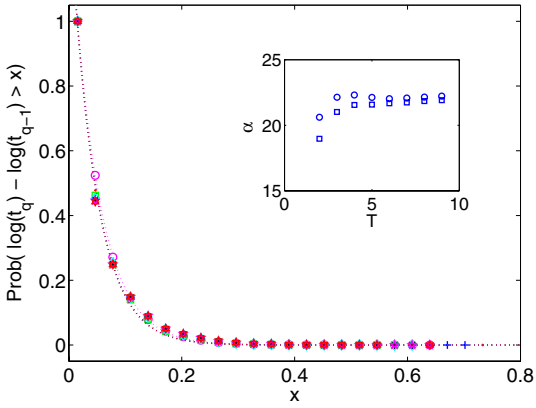

Fig. 3. (Color on line) For eight different temperatures $T = 0.2, 0.3 \ldots 0.9$ (circles, dots, squares, plusses, diamonds, stars, pentagrams, and hexagrams) the estimated cumulative probability $\text{Prob}(\log t_q/t_{q-1} > x)$ is plotted versus x, with t_q, $q = 1, 2 \ldots$ denoting the times at which the quakes occur. The quakes are identified as described in the main text using the filtering parameter value $f = 7$. The dotted lines are fits to the exponential $\exp(-\alpha x)$. The collapse of the eight data sets demonstrates that the temperature dependence is very weak, except at the lowest T. In the insert, the fitted α values are plotted versus T. The circles pertain to the data shown in the main plot, and the squares pertain to corresponding data obtained using $f = 8$ as a filter parameter.

For temperatures $T = 0.2, 0.3 \ldots 0.9$, a range spanning most of the EA spin-glass phase, simulations were performed in the interval $t \in (200, 10200)$. Within each trajectory, quakes are identified by applying equation (2), and the quantities $\tau_q = \log(t_q/t_{q-1})$ are calculated and binned. The procedure is repeated for 2000 independent trajectories for each value of the temperature. The magnetic field $H = 0.1$ for $t > t_w = 200$ and zero otherwise, is the same as in all other simulations. Note that, as also demonstrated by Figure 4, the magnetic field has no discernible effects on the energy statistics. The standard deviation, $\sigma(i)$, of the empirical probability of a point falling in the i'th bin is $\sigma(i) = \sqrt{(p_{th}(i)/N_{obs})}$, where $p_{th}(i)$ is the corresponding (unknown) theoretical probability. N_{obs} is the number of τ_q values collected. Replacing p_{th} with the corresponding empirical probability, yields an estimate for $\sigma(i)$. The empirical cumulative distribution $\text{Prob}(\tau_q = \log(t_q/t_{q-1}) > x)$ is fitted to the exponential $be^{\alpha x}$, with fit parameters obtained by mimizing the sum of the square differences to the data points, each weighted by the reciprocal of the (estimated) variance of the data point. The prefactor b has no physical significance. It would be unity, where not for the fact that the lowest x value, for which the ordinate is equal to one, is located at half bin size, rather than at zero. To check the influence of f on the form of the distribution, all the simulations were done twice, using the values $f = 7$ and $f = 8$. The results shown in the main panel of Figure 3 pertain to the $f = 7$ case. The results for $f = 8$ are very similar, i.e. both cases produce an exponential distribution. The scale parameter α lacks any significant T

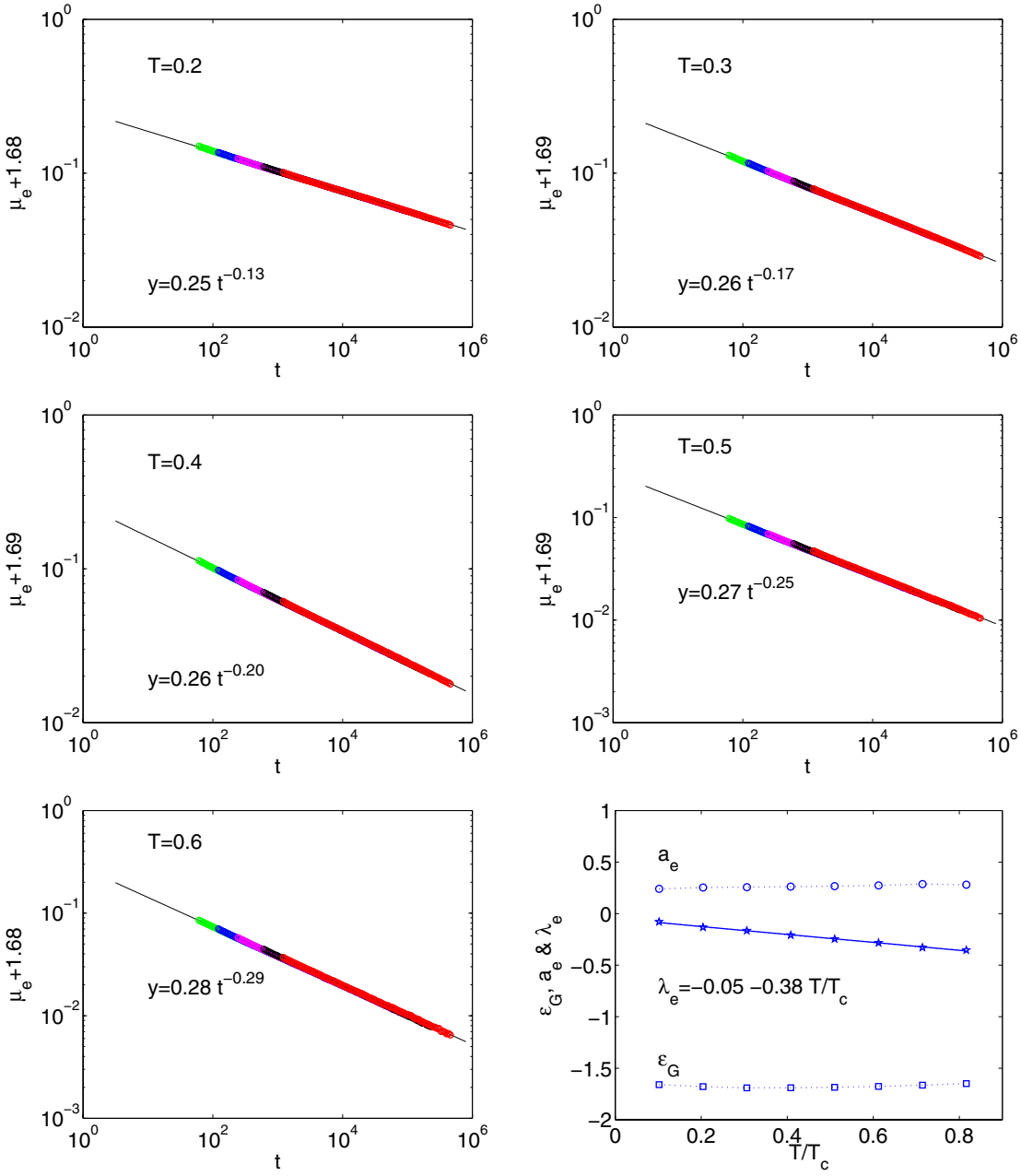

Fig. 4. (Color on line) The first five panels depict, for the temperatures indicated, scaling plots of the energy per spin, with the constant ϵ_G, subtracted. The values of t range from $t = t_w$ to $400t_w$, with $t_w = 50, 100, 200, 500$ and 1000, (green, blue, magenta, black, and red circles respectively). The black line is a fit to equation (4). The value of t_w is irrelevant for the energy decay. The last panel shows the T dependence of the parameters of equation (4) on the reduced temperature T/T_c.

dependence, except for the lowest temperature, and seems only weakly f dependent. From the statistics, the number of domains can be estimated as $\alpha \approx 20$. Dividing the total number of spins by α an order of magnitude estimate is obtained for the number of spins in a thermalized domain. The corresponding linear size comes out around 6 spins, a figures which compares well to the range of domain sizes observed in domain growth studies of the EA model [23]. The scale invariance of the energy landscape implicit in the T independence of α is to a large degree confirmed. It is expected that the largest deviations be found at the lowest temperatures, where the discreteness of the energy spectrum begins to make itself felt.

3.3 Average energy and linear response

The drift of the average energy μ_e and average magnetization μ_{ZFCM} was seen to mainly depend on the number of quakes n_I which fall in the relevant observation interval. For an interval (t, t') this number was shown to have a

Poisson distribution with average

$$\langle n_I \rangle = \alpha \ln(t/t'). \quad (3)$$

For a final check of the applicability of record dynamics we now compare available analytic formulas [13,16] for the average energy, magnetic response and magnetic correlation function to the spin glass data. The subordination hypothesis used to derive the formulas fully neglects the effects of pseudo-equilibrium fluctuations. Then, all observables have a rather simple and generic n_I dependence — a superposition of exponential functions. Averaging over the distribution of n_I produces a superposition of power-laws terms, some of which can be further expanded into a logarithmic and a constant term. The independent variables are t and t/t_w for the energy and the magnetization, respectively, since all quakes contribute to the energy decay, while only those falling between t_w and t contribute to the response.

Because pseudo-equilibrium fluctuations are excluded, deviations between predicted and observed behavior are to be expected. Indeed, as discussed later, the linear response. data have a small additive t_w dependence which is beyond the reach of the description and which is in most studies explicitly split off as a 'stationary contribution [25].

The average energy and linear response are calculated using 4000 independent trajectories. The average energy $\mu_e(t)$ is found to decay toward an (apparent) asymptotic limit ϵ_G, according to the power-law

$$\mu_e(t) - \epsilon_G = a_e t^{\lambda_e}. \quad (4)$$

In the first five panels of Figure 4, the full line corresponds to equation (4) and the symbols are empirical estimates of the average energy. Each panel shows data obtained at the temperature indicated. For each T, the five data sets displayed are for $t_w = 50, 100, 200, 500$ and 1000 (green, blue, magenta, black and red, respectively). The lack of a visible t_w dependence shows that the magnetic contribution to the energy is negligible, as expected. The last panel of Figure 4 summarizes the dependence of ϵ_G and of the decay exponent λ_e on the reduced temperature T/T_c. The estimate $T_c = 0.98$ [30] is used for the critical temperature of the EA model. Interestingly, the fitted value of ϵ_G is nearly independent of T, and is close to the estimated ground state energy of the EA model, [31] $e_G = -1.7003 \pm 0.008$. Equation (4) concurs with the observation that a 'putative' ground state energy of complex optimization problems can be guessed at early times [32,33]. The prefactor a_e has a negligible T dependence. In contrast, the exponent λ_e has a clear linear dependence $\lambda_e = -0.05 - 0.38T/T_c$.

For $\lambda_e \ln t < 1$, the average energy decay is logarithmic, $\mu_e(t) \approx \epsilon_G + a_e + a_e\lambda_e \ln(t) \ldots$, and the decay rate falls off as the inverse of the age [8,15]. The coefficient $a_e\lambda_e$, which receives its temperature dependence from λ_e, is proportional to the average size of a quake [15]. Even though quakes are strongly exothermic, their average size may slightly increase with T. This effect of thermal activation on the size of quakes is analyzed (for a different model) in reference [15].

An excellent parameterization of the average ZFCM time dependence is given by

$$\mu_{ZFCM}(t/t_w) = b_0 + a_m \ln\left(\frac{t}{t_w}\right) + b_m \left(\frac{t}{t_w}\right)^{\lambda_m}. \quad (5)$$

In the theory, the left-hand side should only depend on t/t_w, i.e. b_0 should be constant. However, a small t_w dependent term, the well known stationary part of the response, is present. To be able to nevertheless plot the data versus t/t_w we shift them vertically in a t_w dependent fashion, i.e. we subtract the stationary term. The magnitude of the shift increases with t_w and with T, reaching, at its highest, approximately 15% of the value of b_0 which fits the $tw = 50$ data.

The first five panels of Figure 5 show the average ZFCM (dots) and the corresponding fits (lines) as a function of t/t_w, for $t_w = 50, 100, 200, 500$ and 1000. The simulation temperature used is indicated in each case. Sets of data corresponding to different t_w values are color coded as done for the average energy. The black line is given by equation (5), with its three parameters determined by least square fits. The field switch at t_w has a 'transient' effect described by the power-law decay term: When t/t_w is sufficiently large, the ZFCM increases proportionally to $\ln(t/t_w)$, and hence at a rate decreasing as a_m/t. In the last panel of Figure 5, the decay exponent λ_m and the constants a_m and b_m are plotted versus T. The full line shows the linear fit $-\lambda_m = 1.10 + 0.33T/T_c$, the dotted lines are guides to the eye. Importantly, the constant of proportionality a_m is practically independent of T, a property also shared by a_e. This strongly indicates that the logarithmic rate of quakes, α (see Eq. (3)) must similarly be T independent.

The derivative of μ_{ZFCM} with respect to the logarithm of the observation time, the so-called 'relaxation rate', can be written as

$$S(t_w, t) = (t - t_w)\frac{\partial \mu_{ZFCM}}{\partial t} = (t - t_w) r_{ZFCM}, \quad (6)$$

where r_{ZFCM} is the rate of magnetization increase. The plots of S versus the observation time $t_{obs} = t - t_w$ are produced via equations (5) and (6) and displayed in the inserts of the first five panels of Figure 5. One recognizes the characteristic peak at $t_{obs} = t_w$ [22,34]. The limiting value for $t \gg t_w$ is a_m, i.e. precisely the asymptotic logarithmic rate of increase of the ZFC magnetization.

The sum of the TRM and ZFCM is the field cooled magnetization (FCM). Unlike the ZFCM, both FCM and TRM have a a non-linear H dependence [34]. The latter does not seem to affect the intermittent behavior, at least if numerical simulation data and experimental data can be treated on the same footing: experimental TRM decay data [16] have the same general behavior as the ZFCM data just discussed. However two power-law terms, rather than one, are needed to describe the, more complex, experimental transient. The exponents have ranges similar to λ_m, and a somewhat stronger variation with T. The large t/t_w asymptotic behavior is a logarithmic decay, $a \ln(t/t_w)$, where, importantly, the coefficient of proportionality a is T independent, except for T very close to T_g.

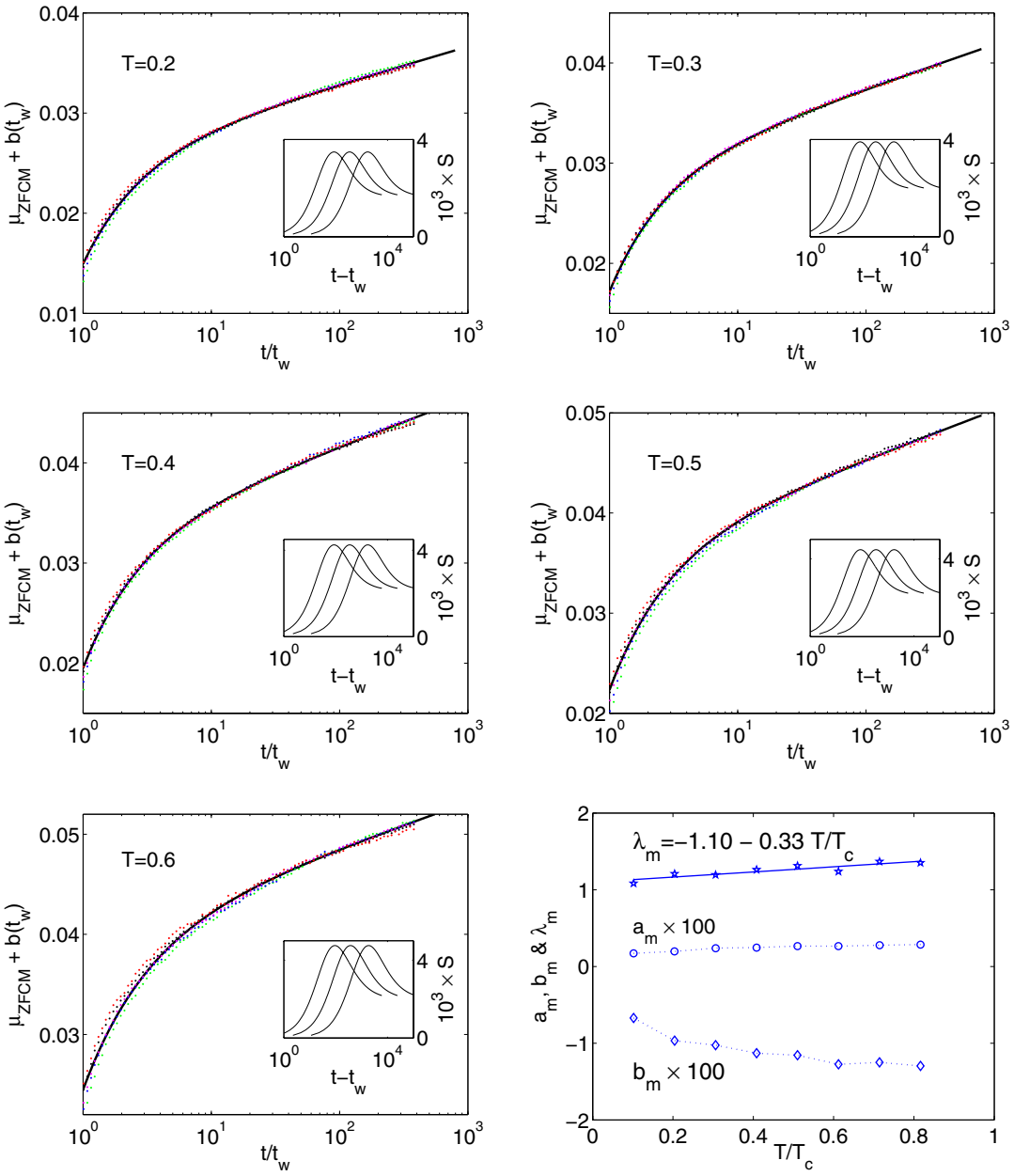

Fig. 5. (Color on line) The first five panels display, for the temperatures indicated, scaling plots of the magnetization with a small t_w dependent quantity $b(t_w)$ added. The abscissa is t/t_w, with t_w equal to $50, 100, 200, 500$ and 1000. The values of t range from $t = t_w$ to $t = 400t_w$. The data are fitted to the sum of a logarithm and a power-law (see Eq. (5)). In the inserts, the relaxation rate S is plotted versus the observation time $t - t_w$. The values of S are obtained by applying equation (6) to the fitted functional form for μ_{ZFCM} given in equation (5). The last panel shows the dependence of the parameters of equation (5) on the reduced temperature T/T_c. The negative of λ_m is plotted for graphical reasons.

With an eye to the following discussion, we recall that the average configuration autocorrelation function of the EA model, normalized to unity at $t = t_w$, decays between times t_w and t as

$$\mu_C(t/t_w) = (t/t_w)^{\lambda_c}\,; \quad t \geq t_w, \tag{7}$$

where the exponent can be fitted to the linear T dependence $\lambda_c(T) = -0.25T/T_c$ [13]. The algebraic decay follows from record dynamics arguments which neglect the effect of quasi-equilibrium fluctuations for $t \approx t_w$. Furthermore, they fail near the final equilibration stages. Note that in the notation of reference [13] the ratio t/t_w is written as $1 + t/t_w$.

4 Discussion and conclusions

In this and a series of preceding papers [8,10,12,13,15,16], we have argued that non-equilibrium events, the quakes, are key elements of intermittency and non-equilibrium aging. The approach takes irreversibility into account at the microscopic level, stressing that thermal properties alone, e.g. free energies, are inadequate to explain non-equilibrium aging. These properties remain nevertheless important in the description, since the record sized (positive) energy fluctuations which are assumed to trigger the quakes are drawn from an equilibrium distribution. As earlier discussed [15], the energy landscape of each domain must be self-similar in order to support a scale invariant statistics of record fluctuations. In this optics, the scale invariance of the 'local' energy landscape attached to each domain, rather than the scale invariance of real space excitations, is at the root the slow relaxation behavior of aging systems [35–37].

A different approach to non-equilibrium aging considers a generalization of the Fluctuation Dissipation Theorem (FDT) [26,38–40]. Its relation to record-dynamics is briefly considered below. Out of equilibrium, the FDT is never fulfilled exactly [41], nor is it generally possible to write the linear response as a function of the conjugate autocorrelation alone. Nevertheless, for time scales $t - t_w \ll t_w$, the drift part of aging dynamics is negligible, and the FDT does, in practice, apply [27]. As mentioned, conjugate response and autocorrelation functions are naturally divided into *stationary* and *non-stationary* parts, which pertain to the pseudo-equilibrium and off-equilibrium aging regimes, respectively. Adopting the standard notation C for the correlation and R for the magnetic response, the FDT reads $(1-C(t))/T = R(t)/H$. For equilibrium data, a plot of C versus $\chi = R/H$ yields a straight line with slope $-1/T$. For aging data, the same plot produces a straight line in the quasi-equilibrium regime, e.g. at early times where C is close to one. Accordingly, a measure of the deviation from quasi-equilibrium is the Fluctuation Dissipation ratio (FDR) [38], which is defined as $X(C) = -Td\chi(C)/dC$. In the case of the EA model, the relation $\ln C = \lambda_c \log(t/t_w)$, which follows from inverting equation (7), can be used to find $\chi(C)$ and to calculate $X(C)$. The latter is nowhere a linear function of C, which is expected, as the stationary fluctuation regime is excluded from the description. The effective temperature [40] is usually defined from the large t and t_w asymptotic limit of the Fluctuation Dissipation ratio. Effective temperatures may depend on the choice of conjugate observables [40], and are not easily measured experimentally [4,39], but offer nevertheless a simple and appealing characterization of aging dynamics.

In a record-dynamics context, fluctuation-dissipation like relations arise out of equilibrium because correlation and response are both subordinated to the same quakes. Due to the monotonicity of their t/t_w dependencies, each of the two can can be written as a function of the other, and a FDR can thus be constructed. Asymptotically, both correlation and response may have an approximate logarithmic dependence on t/t_w: from equation (5), we see that $R(t/t_w) \approx a_m \ln(t/t_w)$ for $t/t_w \gg 1$. Considering that λ_c vanishes for $T \to 0$, we also obtain, for the same range of t/t_w values, the inequality $|\lambda_c(T)| \ln(t/t_w) < 1$. When the inequality is fulfilled, equation (7) can be written as $1 - C(t/t_w) \approx -\lambda_c(T) \ln(t/t_w) \propto R(t/t_w)$. A relation formally similar to the FDT holds, with T replaced by

$$T_{\text{eff}} = \frac{-\lambda_c H}{a_m} = \frac{T}{4T_c(a_m/H)}. \tag{8}$$

As $a_m \propto H$, there is of course no H dependence. Importantly, $T_{\text{eff}} \propto T$, as a_m is independent of T. For the parameter values obtained from the fits, $T_{eff} > T$, even though a general argument to support the inequality is lacking at the moment.

The approach used in this paper and in reference [16] should be generally applicable to check for the presence of record-dynamics features in intermittent fluctuation data. Clearly the ability to perform calorimetry experiments is essential to directly check the temporal statistics of the quakes. In the absence of such data, one may assume that quakes produce large intermittent changes in other observables, and use their statistics instead.

Financial support from the Danish Natural Sciences Research Council is gratefully acknowledged. The bulk of the calculations was carried out on the Horseshoe Cluster of the Danish Center for Super Computing (DCSC). The author is indebted to G.G. Kenning for insightful comments.

References

1. W.K. Kegel, A. van Blaaderen, Science **287**, 290 (2000)
2. E.R. Weeks, J.C. Crocker, Andrew C. Levitt, Andrew Schofield, D.A. Weitz, Science **287**, 627 (2000)
3. H. Bissig, S. Romer, L. Cipelletti, V. Trappe, P. Schurtenberger, Phys. Chem. Comm. **6**, 21 (2003)
4. L. Buisson, L. Bellon, S. Ciliberto, J. Phys.: Condens. Matter. **15**, S1163 (2003)
5. L. Buisson, M. Ciccotti, L. Bellon, S. Ciliberto, in *Fluctuations and noise in materials*, *Proceedings of SPIE*, edited by M.B. Weissman D. Popovic, Z.A. Racz, Vol. 5469, pp. 150–163 (Bellingham, WA, 2004)
6. L. Cipelletti, L. Ramos, J. Phys.: Condens. Matter **17**, R253 (2005)
7. A. Crisanti, F. Ritort, EPL **66**, 253 (2004)
8. P. Sibani, H. Jeldtoft Jensen, EPL **69**, 563 (2005)
9. P. Sibani, P.B. Littlewood, Phys. Rev. Lett. **71**, 1482 (1993)
10. P. Sibani, J. Dall, EPL **64**, 8 (2003)
11. P. Anderson, H. Jeldtoft Jensen, L.P. Oliveira, P. Sibani, Complexity **10**, 49 (2004)
12. P. Sibani, H. Jeldtoft Jensen, JSTAT, 10013 (2004)
13. P. Sibani, EPL **73**, 69 (2006)
14. L.P. Oliveira, H. Jeldtoft Jensen, M. Nicodemi, P. Sibani, Phys. Rev. B **71**, 104526 (2005)
15. P. Sibani, Phys. Rev. E **74**, 031115 (2006)
16. P. Sibani, G.F. Rodriguez, G.G. Kenning, Phys. Rev. B **74**, 224407 (2006)
17. L. Lundgren, P. Svedlindh, P. Nordblad, O. Beckman, Phys. Rev. Lett. **51**, 911 (1983)

18. M. Alba, M. Ocio, J. Hammann, EPL **2**, 45 (1986)
19. V.S. Zotev, G.F. Rodriguez, G.G. Kenning, R. Orbach, E. Vincent, J. Hammann, Phys. Rev. B **67**, 184422 (2003)
20. G.F. Rodriguez, G.G. Kenning, R. Orbach, Phys. Rev. Lett. **91**, 037203 (2003)
21. I.S. Suzuki, M. Suzuki, Phys. Rev. B **68**, 094424 (2003)
22. J.-O. Andersson, J. Mattsson, P. Svedlindh, Phys. Rev. B **46**, 8297 (1992)
23. H. Rieger, J. Phys. A **26**, L615 (1993)
24. J. Kisker, L. Santen, M. Schreckenberg, H. Rieger, Phys. Rev. B **53**, 6418 (1996)
25. F. Ricci-Tersenghi M. Picco, F. Ritort, Eur. Phys. J. B **21** 211 (2001)
26. H.E. Castillo, C. Chamon, L.F. Cugliandolo, J.L. Iguain, M.P. Kenneth, Phys. Rev. B **68**, 13442 (2003)
27. E. Vincent, J. Hammann, M. Ocio, J. Bouchaud, L.F. Cugliandolo, SPEC-SACLAY-96/048 (1996)
28. J. Dall, P. Sibani, Comp. Phys. Comm. **141**, 260 (2001)
29. P. Nordblad, K. Gunnarsson, P. Svedlindh, L. Lundgren, R. Wanklyn, J. Magn. and Magnetic Materials **71**, 17 (1987)
30. G. Parisi E. Marinari, J.J. Ruiz-Lorenzo, Phys. Rev. B **58**, 14852 (1998)
31. K.F. Pal, Physica A **233** 60 (1996)
32. P. Sibani, J.M. Pedersen, K.H. Hoffmann, P. Salamon, Phys. Rev. A **42**, 7080 (1990)
33. R. Tafelmayer, K.H. Hoffmann, Comput. Phys. Comm. **86**, 81 (1995)
34. C. Djurberg, J. Mattsson, P. Nordblad, EPL **29**, 163 (1995)
35. P. Sibani, K. Heinz Hoffmann, Phys. Rev. Lett. **63**, 2853 (1989)
36. P. Sibani, C. Schön, P. Salamon, J.-O. Andersson, EPL **22**, 479 (1993)
37. R. Orbach Y.G. Joh, J. Hammann, Phys. Rev. Lett. **77**, 4648 (1996)
38. L.F. Cugliandolo, J. Kurchan, L. Peliti, Phys. Rev. E **55**, 3898 (1997)
39. D. Hérisson, M. Ocio, Phys. Rev. Lett. **88**, 257202 (2002)
40. P. Calabrese, A. Gambassi, J. Phys. A **38**, R133 (2005)
41. G. Diezemann, Phys. Rev. E **72**, 011104 (2005)